Glutathione induces Arabidopsis *PHT1;5* gene via WRKY75 transcription factor to regulate phosphate homeostasis

Ranjana Shee[1,2], Dibyendu Shee[1,2,], Salman Sahid[1,2,3],Soumitra Paul[1*], Riddhi Datta[2*]

[1]Department of Botany, University of Calcutta, 35, Ballygunge Circular Road, Kolkata 700019, West Bengal, India

[2]Department of Botany, Dr A. P. J. Abdul Kalam Government College, New Town, Kolkata 700156, West Bengal, India

[3]Present address: Department of Botany, Acharya Prafulla Chandra Roy Government College, Himachal Bihar Phase 1, Matigara, Siliguri, West Bengal, India

*****Authors for correspondence:

SP and RD should be considered as senior authors

Email: psoumitra@ymail.com,riddhi.bot@gmail.com; Telephone No: +919748605305, +919433084074

ORCID IDs:

RiddhiDatta: 0000-0001-7490-190X

Soumitra Paul: 0000-0001-7560-5512

Running head: GSH regulates phosphate homeostasis via *At*PHT1;5 transporter

Funding

This work has been supported by the Science and Engineering Research Board, Government of India [ECR/2017/000231] and Start up Grant, University Grant Commission, Government of India, India [F30-363/2017(BSR)]

Keywords: Glutathione, phosphate deficiency, phosphate transport, PHT1;5, WRKY75

Summary statement

Glutathione regulates phosphate translocation in Arabidopsis under altered phosphate condition via transcriptional activation of *AtPHT1;5* gene by *At*WRKY75 transcription factor.

Abstract

Phosphorus is a macronutrient that regulates a wide range of physiological processes, including plant growth and development. The scarcity of bioavailable phosphate is often a constraint for plant growth in most agricultural ecosystems. Under phosphate limited conditions, plants increase phosphate acquisition or alter its distribution within tissues by activating different phosphate transporters and phosphate starvation-induced genes. Glutathione (GSH), on the other hand, is known to play a critical role in regulating iron and zinc homeostasis in Arabidopsis. However, how it regulates phosphate homeostasis under phosphate limited conditions remains unexplored. We found that the two GSH-deficient mutants, *cad2-1*, and *pad2-1*, were hypersensitive to phosphate starvation. Under phosphate-sufficient condition, the root phosphate content was lower in the mutants but significantly higher in the shoot over the Col-0 plants. The pattern was reversed under phosphate-deficient condition. Interestingly, among the different phosphate transporters analyzed, the *AtPHT1;5* was significantly down-regulated in the two GSH-deficient mutants. Treatment with exogenous GSH could alter phosphate accumulation in Col-0 and the *pht1;5* complementation lines but not in the *pht1;5* mutant. This observation confirmed the role of GSH in phosphate reallocation during phosphate starvation via the *At*PHT1;5 transporter. Further, promoter analysis demonstrated that GSH regulates the transcription of the *AtPHT1;5* gene. The phosphate-responsive transcription factor (TF), *At*WRKY75 was identified to interact with the *AtPHT1;5* promoter, and phosphate deficiency or GSH treatment enhanced its binding affinity. Together our investigation delineates that GSH regulates the *At*PHT1;5 transporter via the *At*WRKY75 TF to modulate phosphate distribution under altered phosphate conditions.

Introduction

Phosphorous (P) is an essential macronutrient that regulates various physiological phenomena in plants. It serves as a crucial component of nucleic acids, phospholipids, and different sugar-phosphate intermediates. Moreover, the phosphorylation of regulatory proteins and enzymes plays a critical role in modulating various signal transduction pathways (Poirier and Bucher, 2002). In plants, inorganic phosphate (Pi) is the primary source of P taken up by the roots from the soil. However, Pi is poorly available to plants due to its high reactivity with soil calcium, aluminum, or iron (Fe), leading to its precipitation or incorporation into organic compounds (Bieleski, 1973). Therefore, Pi-deficiency is a severe constraint for plant growth and development. Plants have evolved intricate mechanisms to improve the uptake and utilization of Pi from the rhizosphere as well as to reallocate the internal Pi reserve for maintaining P homeostasis under Pi-limited conditions. P deficiency alters root system architecture (RSA), impairs photosynthesis, triggers the synthesis of acid phosphatases (APases), ribonucleases, and organic acids, and induces anthocyanin and starch accumulation in plants (Vance et al., 2003). Since the concentration of Pi in a plant cell is 10^2-10^3 times higher than that in the soil, plants transport Pi against the concentration gradient with the help of different low and high-affinity P transporters (Shin et al., 2004). Earlier, three important P transporter families, *viz.* phosphate transporter (PHT) family, SYG1/Pho81/ XPR1 (SPX) domain-containing protein family, and sulfate transporter (SULTR)-like family, were reported in plants (Liu et al., 2017). Among them, the PHT family transporters, which play a crucial role in Pi acquisition and P allocation, are categorized into five groups based on their subcellular localization (Liu et al., 2016). For example, PHT1 localizes on the plasma membrane, while PHT2 and PHT4 are on the chloroplast membrane. On the other hand, PHT3 and PHT5 localize on mitochondrial and vacuolar membranes, respectively.

The PHT1 family of P transporters comprises nine members in Arabidopsis, located on the chromosomes 1, 2, 3, and 5 (Mudge et al., 2002). Interestingly, four PHT1 family genes, *PHT1;1*, *PHT1;2*, *PHT1;3*, and *PHT1;6*, are clustered on chromosome 5, indicating a gene duplication during the evolution of the PHT1 family in the Arabidopsis genome (Mudge et al., 2002). The family functions as H^+/Pi symporters during Pi uptake from the soil and its distribution within plants (Zhang et al., 2014). The PHT1;1 plays a dominant role in Pi uptake from the rhizosphere under high P conditions, while PHT1;4 predominantly helps in Pi acquisition under P-limited conditions. Besides, PHT1;2, PHT1;3, and PHT1;5 also function

in Pi uptake from soil (Shin et al., 2004; Nagarajan et al., 2011; Ayadi et al., 2015). Apart from Pi acquisition by roots, P allocation and transport to different tissues are also crucial for P homeostasis in plants. The PHT1;8 and PHT1;9 transporters function in root-to-shoot P translocation in co-operation with the PHO1, PHT1;3 and PHT1;4 (Mudge et al., 2002; Lapis-Gaza et al., 2014). Furthermore, P rescue from senescing leaves offers a way for recycling P reserves in plants. PHT1;5 is vital to the process. Similarly, the PHT1;5 transporter is implicated in P redistribution from source to sink tissues in response to developmental signals and P status in the soil (Nagarajan et al., 2011). Although Pi deprivation dramatically increases the expression of several PHT1 genes, others are expressed irrespective of the soil Pi concentration. The low Pi signal is often transduced by several P-responsive transcription factors (TFs) like PHOSPHATE STARVATION RESPONSE 1 (PHR1), WRKY, and MYB domain-containing families to activate specific PHT1 transporters (Rubio et al., 2001; Gu et al., 2016). Tight control of P transporters allows efficient Pi use in plants during P deficiency.

Glutathione (GSH) is a ubiquitous tripeptide that serves as a master regulator of plant growth, development, and stress response. It functions in reactive oxygen species (ROS) detoxification, redox homeostasis, and defense signaling network under various biotic and abiotic stress conditions (Foyer and Noctor, 2011; Noctor et al., 2012). In addition, GSH can impart tolerance to different metal toxicity in plants by activating phytochelatin synthesis (Seth et al., 2012; Jozefczak et al., 2014). Several GSH-deficient Arabidopsis mutants with varying levels of susceptibility to biotic and abiotic stress factors have been identified. Among them, the *cadmium sensitive 2-1* (*cad2-1*) mutant displays severe sensitivity to cadmium and possesses around 30% GSH content than that in wild-type plants (Howden et al., 1995). On the other hand, the *phytoalexin deficient2-1* (*pad2-1*) mutant containing 22% GSH exhibits susceptibility to different pathogen infections (Glazebrook and Ausubel, 1994; Parisy et al., 2007).

GSH is also involved in modulating nutrient homeostasis in Arabidopsis. For example, the *zir1* mutant that contains 15% GSH displayed increased sensitivity to Fe-limited conditions (Shanmugam et al., 2012). During Fe deficiency, GSH maintains the redox homeostasis in the cell and increases the uptake and accumulation of Fe by activating different Fe-responsive genes like *FRO2*, *FIT1*, and *IRT1* in Arabidopsis (Shanmugam et al., 2015). Earlier, we reported that the GSH-(S-nitrosoglutathione) GSNO module regulates

subcellular Fe homeostasis by modulating *At*NRAMP3, *At*NRAMP4, and *At*PIC1 transporters during Fe deficiency (Shee et al., 2022). However, the role of GSH in modulating the P transport or homeostasis remains unexplored. Although GSH-indole butyric acid (IBA) crosstalk was reported to alter the RSA under Pi-deprived condition, the mechanism of GSH-mediated P homeostasis is not elucidated (Trujilo Hernandez et al., 2020). Here we demonstrate that GSH modulates source to sink P transport via transcriptional activation of the *AtPHT1;5* transporter through the *At*WRKY75 TF under altered Pi conditions.

Results

GSH-deficient mutants display sensitivity to Pi deprivation

To understand if GSH plays any role in regulating P homeostasis, we analyzed the response of the GSH-deficient mutants, *cad2-1*, and *pad2-1*, along with the wild-type (Col-0) plants under Pi-deprived condition. The standard Murashige and Skoog (MS) medium (1.25mM KH_2PO_4; +P) was used as a Pi-sufficient medium, while the Pi-deficient medium (0mM KH_2PO_4; 0.5 mM K_2SO_4; -P) lacked any Pi source. Under the Pi-sufficient condition, neither *cad2-1* nor *pad2-1* showed any phenotypic alteration compared to the Col-0 plants. In response to 7 d of Pi starvation, all three genotypes displayed smaller rosettes, shorter primary roots, and increased lateral root density compared to the Pi-sufficient condition. The *pad2-1* mutant, however, exhibited severe sensitivity to Pi deficiency with a reduced rosette diameter, lower lateral root number, and density over the Col-0 plants (Fig. 1A-E). Although the chlorophyll content dropped in all three genotypes in response to Pi deficiency, the drop was sharper in *pad2-1* (Fig. 1F). On the contrary, the increase in the anthocyanin content under Pi-deprived condition was significantly lower in both *cad2-1* and *pad2-1* compared to the Col-0 plants (Fig. 1G).

To assess any possible P-GSH interplay, we estimated the GSH, Pi and total P contents under Pi-sufficient and Pi-deficient conditions. Under Pi-sufficient condition, the root Pi and total P contents were significantly lower in both *cad2-1* and *pad2-1* mutants. In response to Pi deprivation, however, the *pad2-1* mutant displayed a higher root Pi and total P accumulation over the *cad2-1* and Col-0 plants (Fig. 2A, B). In addition, the total root GSH content increased, but the GSH:GSSG ratio decreased in all three genotypes when exposed to Pi starvation (Fig. 2C-D). Although the total GSH content increased and GSH:GSSG ratio decreased under the Pi-limited condition in the shoot, the Pi and total P status displayed a

contrasting pattern (Fig. 2E-H). The shoot Pi and total P contents were significantly higher in the mutants under the Pi-sufficient condition, but lower under the Pi-deficient condition.

GSH regulates AtPHT1;5 to modulate P transport

The sensitivity of the GSH-deficient mutants to Pi starvation and their altered P status prompted us to investigate if GSH can regulate any P transporter genes. To this end, we analyzed the expression of several known P transporters from the root and the shoot under Pi-sufficient condition and compared their relative transcript abundance between the Col-0 and the GSH-deficient mutants. Interestingly, the *AtPHT1;5* expression was significantly down-regulated in both the mutants compared to the Col-0 plants (Fig. 3A-B). Although Pi deficiency induced the *AtPHT1;5* expression in all three genotypes, its transcript abundance was significantly lower in the mutants than the Col-0 plants (Fig. 3C-D).

Further, we examined the *AtPHT1;5* expression in the Col-0 plants under exogenously altered GSH conditions. The total GSH content increased in response to exogenous GSH treatment, while the GSH biosynthesis inhibitor, buthionine sulphoximine (BSO), decreased it. However, treatment with the non-specific reducing agent, dithiothreitol (DTT), did not alter the total GSH content (Fig. 3E, I). Interestingly, the root Pi and total P content increased significantly in response to GSH treatment but decreased when treated with BSO (Fig. 3F, G). The shoot, on the other hand, displayed an opposite pattern (3J, K). However, the treatment with DTT failed to alter the P content in both the root and the shoot. In line with this observation, the *AtPHT1;5* expression was up-regulated in response to GSH treatment and down-regulated by BSO treatment, while DTT did not alter its expression in root as well as shoot (Fig. 3H, L).Further, we treated the GSH-deficient *pad2-1* mutant with exogenous GSH as well as DTT. While the total GSH content increased upon GSH treatment, no significant alteration was observed for DTT treatment. In response to exogenous GSH, the Pi and total P contents increased in roots but decreased in shoots indicating a role of GSH in modulating P homeostasis (Fig S1). In addition, *AtPHT1;5*expression was induced by the GSH treatment while DTT treatment could not alter its transcript abundance (Fig S1).Together, these observations strongly suggest a GSH-mediated regulation of P transport through the *AtPHT1;5* transporter.

GSH modulates P mobilization during Pi starvation by regulating AtPHT1;5 expression

To further examine the role of GSH in regulating P mobilization, we analyzed the response of the *pht1;5* mutant to exogenous GSH treatment. We generated complementation (*pht1;5/pPHT1;5::PHT1;5*) lines harboring the *AtPHT1;5* gene under the control of its native promoter in the *pht1;5* mutant background and analyzed them (Fig. 4A). The Col-0, *pht1;5* mutant, and complementation lines displayed similar total GSH contents, which increased in response to Pi starvation. When treated with exogenous GSH, the total GSH content increased in all three genotypes under both Pi-sufficient and Pi-deficient conditions (Fig. 4B, E). Notably, the *pht1;5* mutant displayed altered root-to-shoot P allocation under both Pi-sufficient and Pi-deficient conditions. When grown under Pi-sufficient conditions, the *pht1;5* mutant accumulated lower Pi and P contents in the root but higher accumulation in the shoot compared to the Col-0 plants. However, under Pi-deficient conditions, it displayed a higher Pi and P accumulation in the root but lower levels in the shoot. The complementation lines, on the contrary, showed similar Pi and P contents as that of the Col-0 plants (Fig. 4C, D, F, G). Fascinatingly, exogenous GSH treatment could enhance Pi and P contents in the root of the Col-0 and the complementation lines under Pi-sufficient condition but slightly reduced it during Pi starvation. In the shoot, the Pi and P contents decreased in response to GSH supplementation under the Pi-sufficient condition, while it increased under Pi deficiency. On the contrary, exogenous GSH treatment could not alter the root and the shoot Pi and P contents of the *pht1;5* mutant under both Pi-sufficient and Pi-deficient conditions (Fig. 4C,D,F,G). This observation strongly suggests that GSH is involved in modulating root-to-shoot P allocation through the *At*PHT1;5 transporter to regulate P homeostasis during Pi starvation.

GSH modulates the transcriptional activation of AtPHT1;5 gene

Since GSH could modulate P allocation via the *AtPHT1;5* transporter, the next pertinent question was how GSH modulates the *AtPHT1;5* expression. To gain a deeper insight, we cloned the *AtPHT1;5* promoter (*pPHT1;5*) and raised transgenic Arabidopsis lines harboring the *pPHT1;5*::*GUS* construct in the background of Col-0. A transgenic line containing the *CaMV35S::GUS* construct served as a negative control. Promoter analysis by histochemical GUS assay demonstrated that the *AtPHT1;5* promoter activity was strongly induced in response to Pi starvation, indicating its P-responsive nature. Interestingly, exogenous GSH treatment also significantly enhanced the GUS activity in this transgenic line indicating the role of GSH in modulating *AtPHT1;5* promoter activity (Fig. 5A). In line with

this observation, the *GUS* gene expression was also strongly up-regulated in response to both Pi starvation and exogenous GSH treatment (Fig. 5B). However, both conditions did not alter the GUS activity and expression in the transgenic line harboring the *CaMV35S::GUS* construct (Fig. 5C-D). This observation demonstrated that the GSH-mediated regulation of *AtPHT1;5* occurs at the transcriptional level.

GSH regulates AtPHT1;5 expression via AtWRKY75 TF

GSH cannot directly bind to the promoter to regulate transcription. Therefore, we were curious if any TF is involved in the process. Several WRKY and MYB TFs, like *At*WRKY6, *At*WRKY42, *At*WRKY45, *At*WRKY75, *At*MYB2, and *At*MYB62, are known to regulate Pi-responsive genes in Arabidopsis. We performed yeast one-hybrid (Y1H) assay to check if these TFs can interact with the *AtPHT1;5* promoter and regulate its transcription. We observed that the *At*WRKY42, *At*WRKY75, and *At*MYB2 could bind to the *AtPHT1;5* promoter, while others did not (Fig. 6A). Next, we wondered if all these three TFs were involved in the GSH-mediated regulation of *AtPHT1;5* under Pi-deficient condition. Interestingly, we found that among these TFs, only the *AtWRKY75* expression was down-regulated in the GSH-deficient mutants, *cad2-1*, and *pad2-1* (Fig. 6B). We further analyzed the relative transcript abundance of the *AtPHT1;5* gene in the mutants of the three TFs under Pi-sufficient and Pi-deficient conditions. Supporting our previous observation, the *AtPHT1;5* expression was induced in response to Pi starvation in the Col-0, *wrky42*, and *myb2* mutants but not in the *wrky75* mutant (Fig. 6C). This observation strongly indicated that the *At*WRKY75 TF is essential for the Pi-responsiveness of the *AtPHT1;5* gene. The dual luciferase transactivation assay further confirmed the *AtPHT1;5* promoter activation by the *At*WRKY75 TF (Fig. 6D). We next aimed to identify the region in the *AtPHT1;5* promoter where *At*WRKY75 specifically binds. *In silico* analysis revealed the presence of three w-box (TTGAC[CT]) motifs in the *AtPHT1;5* promoter region at -99, -176, and -201 positions (Fig. S2). Chromatin immunoprecipitation (ChIP)-qPCR assay confirmed the binding of the *At*WRKY75 TF to the w-box regions of the *AtPHT1;5* promoter with an enhanced binding affinity in response to Pi deficiency or exogenous GSH treatment (Fig. 6E). Next, we wanted to analyze the *AtPHT1;5* promoter activity when the *At*WRKY75 TF was absent. Therefore, we expressed the *pPHT1,5::GUS* construct in the background of the *wrky75* mutant. A *CaMV35S::GUS* construct in the same background served as a negative control. We observed that neither Pi starvation nor exogenous GSH treatment could induce the *AtPHT1;5* promoter

activity as evident from the histochemical GUS activity or *GUS* gene expression (Fig. 6F-G). Together these observations strongly suggest that the GSH-mediated transcriptional induction of *AtPHT1;5* occurs via the *At*WRKY75 TF.

Discussion

Over the last decade, accumulating evidence has revealed that GSH can regulate the transport and homeostasis of several nutrients like Fe and zinc in plants (Shanmugam et al., 2011; Shanmugam et al., 2015; Shee et al., 2021). A recent report has further demonstrated its role in regulating root hair growth under P deficiency via an IBA-dependent pathway (Trujilo-Hernandez et al., 2020). However, no comprehensive investigation has been conducted to date to examine the precise mechanism of how GSH regulates P acquisition or reallocation in plants. In this study, we discovered that GSH regulates the root and shoot P contents in Arabidopsis, depending on the Pi availability.

The two GSH-deficient mutants, *cad2-1*, and *pad2-1* exhibited hypersensitivity to Pi deprivation with alterations in their RSA (Fig.1A-E). Changes in RSA are an adaptive strategy for plants under Pi-limited conditions (Peret et al., 2014). Low Pi availability promoted lateral root growth over primary root by boosting lateral root density and length and limiting primary root growth by reducing cell elongation (Williamson et al., 2001). The *pad2-1* mutant, that contains only 22% GSH, exhibited severe sensitivity to Pi deficiency with reduced lateral root density and rosette diameter compared to the wild-type. Another characteristic P deficiency response is a change in pigment composition, which includes chlorophyll degradation and elevated anthocyanin accumulation (Marschner, 2012; Hernández and Munné-Bosch, 2015). With the reduction in photosynthesis rates, the P-deficient plants have evolved to sustain photo-oxidative stress through anthocyanin accumulation (Hernández and Munné-Bosch, 2015). In this study, the GSH-deficient mutants displayed lower anthocyanin accumulation under Pi-deficient conditions than the wild type, indicating enhanced sensitivity (Fig.1G). The chlorophyll loss under Pi deprivation was also maximal in the *pad2-1* mutant (Fig.1F).These observations resemble an earlier report where the*cad2-1* displayed increased sensitivity to Pi depletion (Trujilo-Hernandez et al., 2020), indicating that the optimum GSH level is essential for adaptation under Pi-limited conditions.

Plants have various P transport mechanisms comprising different high- and low-affinity transporters that allow P acquisition and distribution within the plant. Since the source and

sink relationships are continually changing depending on the developmental stage and P availability, the P transport in plants is an elaborate and complex process (Raghothama, 1999; Bucher et al., 2001). To analyze if GSH can regulate P acquisition or distribution in plants, we measured the Pi and total P content from the GSH-deficient mutants and the wild-type under Pi-sufficient and Pi-deficient conditions. Under Pi-sufficient conditions, both *cad2-1* and *pad2-1* mutants displayed higher P accumulation in shoots but lower P content in roots over the wild-type. The results were, however, reversed under Pi-deficient conditions (Fig. 2). Exogenously altering GSH content in the Col-0 plants resulted in a similar P distribution pattern, confirming our previous observation (Fig 3).These observations suggested a plausible role of GSH in modulating the P reallocation between roots and shoots based on the Pi availability status. Several P transporters are known to regulate P homeostasis through P translocation and redistribution in plants (Mudge et al., 2002; Shin et al., 2004; Nagarajan et al., 2011; Lapis-Gaza et al., 2014). Our experiments identified that GSH regulates the expression of the *AtPHT1;5* under Pi sufficient and Pi deficient conditions (Fig.3). Among the PHT1 members, PHT1;5 is expressed exclusively in phloem cells of older leaves, cotyledons, and flowers during P starvation (Mudge et al., 2002). Another genome-wide transcriptome study reported the *PHT1;5* expression in the senescent Arabidopsis leaves (van der Graaff et al., 2006). Intriguingly, PHT1;5 plays a pivotal role in transporting P from the source to the sink organs in response to developmental signals and P availability. During Pi starvation, the loss-of-function mutation of the *PHT1;5* gene resulted in decreased P allocation to shoots, while under Pi-replete conditions, the mutant exhibited higher shoot P content over the wild type but lower P content in the roots (Nagarajan et al., 2011). Notably, the GSH-deficient mutants in our investigation displayed a strikingly similar P distribution pattern with that of the *pht1;5* mutant. We hypothesized that the GSH-mediated modulation of source-to-sink P allocation involves the PHT1;5 transporter. To test this hypothesis, we measured the Pi and total P content of the *pht1;5* mutants and its complementation lines under Pi-sufficient and Pi-deficient conditions in response to exogenous GSH treatment. Under both Pi-sufficient and Pi-deficient conditions, exogenous GSH altered the root and shoot P contents in the wild-type and complementation lines. However, the P content in the *pht1;5* mutants remained unchanged (Fig.4). These findings strongly suggest that GSH not only regulates the expression of the *AtPHT1;5* gene, but also integrates the source-to-sink P allocation mechanism via this transporter in accordance with the P availability status.

The next pertinent question is how GSH regulates the *AtPHT1;5* expression. Since GSH alters the relative transcript abundance of the transporter, transcriptional regulation is the most likely reason. Our experiments demonstrated that the *AtPHT1;5* promoter is inducible under Pi-deficient conditions. The promoter activity is also induced in response to exogenous GSH treatment indicating a GSH-mediated transcriptional regulation of the *AtPHT1;5* gene (Fig.5). However, being a metabolite GSH cannot directly interact with the promoter to modulate its activity. Therefore, we were curious if any TF is involved in the process. Earlier reports suggested that GSH can activate different promoters via their TF (Shee et al., 2022). For example, GSH can modulate ethylene biosynthetic pathway genes via the WRKY33 TF (Datta et al., 2015). In another study, we reported that under Fe-limited conditions, GSH can regulate the *NRAMP3/4* and *PIC1* genes via *S*-nitrosylation of Fe-responsive bHLH TFs (Shee et al., 2022). Several TFs are reported to regulate the expression of different P starvation-induced genes. Previously, it was reported that the WRKY6 and WRKY42 TFs function as repressors of the P transporter, PHO1 (Chen et al., 2009). Under low P conditions, these TFs are degraded, allowing the expression of the *PHO1* gene and subsequent regulation of P homeostasis. WRKY75 has long been known to regulate P acquisition and root development in plants (Devaiah et al., 2007). Another TF, WRKY45 can directly bind to the w-box of the *PHT1;1* promoter to activate its expression under Pi-limited conditions (Wang et al., 2014). Among the different MYB TFs, MYB2 and MYB62 play a crucial role in regulating P starvation response. While MYB2 directly interacts with the promoter of miR399, a marker of P starvation response, MYB62 regulates the Pi starvation response via the gibberellic acid-mediated signaling pathway (Devaiah et al., 2009; Baek et al., 2013). In the present investigation, *At*WRKY42, *At*WRKY75, and *At*MYB2 were identified to interact with the *AtPHT;5* promoter. Among these three TFs, the *AtPHT1;5* expression was significantly lower in the *wrky7*5 mutant (Fig.6). This data corroborates the previous report where *AtPHT1;5* expression was diminished in the wrky75-RNAi lines under both P-sufficient and P-deficient conditions (Nagarajan et al., 2011). Moreover, the *AtWRKY75* expression was significantly down-regulated in the GSH-deficient *pad2-1* mutant, which supports the previous report where GSH treated Col-0 leaves displayed higher WRKY75 expression over the control condition (Sinha et al., 2014). We have further demonstrated that the *At*WRKY75 binds to the w-box motifs on the *AtPHT1;5* promoter and its binding affinity increases in response to Pi starvation or GSH treatment (Fig.6). These data delineate that GSH induces *AtPHT1;5* expressions under Pi-deficient condition via the *At*WRKY75 TF (Fig 7).

In summary, it can be concluded that GSH is highly accumulated during Pi starvation to regulate the P translocation in plants. This regulation involves the GSH-mediated transcriptional activation of *AtPHT1;5* transporter via the P-responsive *At*WRKY75 TF.

Materials and Methods

Plant growth and stress treatment

Seeds of *Arabidopsis thaliana* Columbia ecotype (Col-0), that served as wild-type, and two GSH-deficient mutants, *cad2-1* (N68137), and *pad2-1* (N3804), as well as*pht1;5*mutant (N574836) were procured from Nottingham Arabidopsis Stock Centre, UK. Seeds of *myb2* (SALK_043075), *wrky42* (SALK_049063), and *wrky75* (CS121513) mutants were procured from Arabidopsis Biological Resource Centre, USA. Seeds were surface sterilized with 4% sodium hypochlorite and Tween20 and germinated on a standard MS medium. Plants were maintained in a growth chamber at 21±2°C, 60% relative humidity with the photoperiod of 16 h light/8 h dark cycles as standardized before (Datta et al. 2015). For stress treatment, 7 d old seedlings were transferred to Pi sufficient (1.25 mM KH_2PO_4, +P) or Pi deficient (0 mM KH_2PO_4, supplemented with 0.5 mM K_2SO_4, -P) media and maintained for 7 d. After the stress treatment, the plants were photographed and morphological parameters, *viz*. primary root length, lateral root number, lateral root density, and rosette diameter were analyzed using Image J software.

Estimation of Pi and total P content

Pi levels were determined using ammonium molybdate method following Lapis-Gaza et al. (2014) from root and shoot tissues collected under Pi-sufficient or Pi-deficient conditions. Briefly, fresh tissues were homogenized in 1% (v/v) acetic acid and centrifuged at 12,000 g for 15 min at 4□. The supernatant was diluted and mixed with 0.35% (w/v) ammonium molybdate, 1.4% (w/v) ascorbic acid in 1 N sulphuric acid and incubated at dark for 1 h. The absorbance was measured at 820 nm using Double Beam UV-Vis Spectrophotometer (Hitachi). The Pi concentration was determined from the standard curve prepared by the dilutions of KH_2PO_4.

The total P content was also measured by ammonium blue method following Nagarajan et al. (2011). Briefly, root and shoot tissues were dried in hot air oven at 70□ for 2 days and dried samples were weighed and used to prepare ash by heating at 500□ for 3 h. The ash was

dissolved in concentrated hydrochloric acid. The sample was then diluted, mixed with 0.35% (w/v) ammonium molybdate solution and incubated at 45□ for 20 min. The optical density was measured at 820 nm.

Estimation of chlorophyll and anthocyanin contents

Total chlorophyll was estimated from the samples by homogenizing 200mg tissue in 80% acetone, followed by centrifugation at 5000g for 5 min. The total chlorophyll content was determined following Lichtenthaler (1987). Anthocyanin content was estimated according to Matsui et al. (2004). Briefly, samples were homogenized in liquid nitrogen and resuspended in 5 volumes of 45% methanol and 5% acetic acid (v/v). Following centrifugation at 5000 g for 5 min, absorbance was measured at 530 nm and 637 nm using Double Beam UV-Vis Spectrophotometer (Hitachi) and anthocyanin content was calculated.

Estimation of total GSH content and determination of GSH:GSSG ratio

Reduced GSH content was estimated by 5,5'-dithiobis-(2-nitrobenzoic acid) (DTNB) method as described by Anderson (1985). Briefly, 200 mg of tissue was homogenized in 5% sulphosalicylic acid and centrifuged at 12000 g for 20 min. The supernatant was allowed to react with 50 µM DTNB in reaction buffer [0.1 M phosphate buffer (pH 7) and 0.5 mM EDTA] for 5 min and optical density was measured at 412nmusing a Double Beam UV-Vis Spectrophotometer (Hitachi). For estimation of total GSH, 0.4 mM NADPH and 1 U glutathione reductase were added and incubated for 20 min. The optical density was measured at 412nm.The amount of GSSG was determined by subtracting the amount of reduced GSH from the total GSH.

RNA extraction and quantitative-RT PCR analysis

Trizol method was used for isolation of total RNA from samples. The complementary DNA (cDNA) was prepared using iScript™ cDNA Synthesis Kit (Bio-rad) as per manufacturer's protocol. Quantitative PCR amplification was performed using theCFX96 Touch™ Real-Time PCR Detection System (Bio-rad) using iTaq™ Universal SYBR® Green Supermix (Bio-rad) and gene specific primers. *AtActin*2 was used as a reference gene for normalization.

Chemical treatment of seedlings

15 d old seedlings were separately treated with freshly prepared 100µM GSH or 1mM BSO for 72 h or with 5mM DTT for 24 h as standardized before (Shee et al., 2022).

Vector construction and raising of Arabidopsis transgenic lines

The genomic DNA was extracted from Col-0 plants following CTAB method. The 1500 bp sequence upstream of the +1 site of *AtPHT1;5* gene was PCR amplified using specific primers and cloned into*pCAMBIA1304* vector between *BglII* and *BamHI* restriction enzyme (RE) sites to generate *pPHT1;5*::*GUS* construct. The coding sequences of the*AtPHT1;5* and *AtWRKY75* genes were PCR amplified from cDNA using gene specific primers. The amplified *AtPHT1;5* gene was cloned into *pBI121*vector between *BamHI* and *SacI* RE sites to produce the *CaMV35S*::*PHT1;5* construct. The PCR amplified *AtPHT1;5* promoter was further sub-cloned into the recombinant *CaMV35S*::*PHT1;5* vector between *SphI* and *BamHI* RE sites to generate *pPHT1;5::PHT1;5* construct. The amplified *AtWRKY75* gene was cloned into *pVYCE* vector under control of the *CaMV35S* promoter between *SpeI* and *BamHI* RE sites to generate *CaMV35S::WRKY75-HA* construct. The recombinant *pPHT1;5*::*PHT1;5* construct was used for *Agrobacterium*-mediated genetic transformation of *pht1;5* mutant to raise the complementation lines whereas *CaMV35S::WRKY75-HA* construct was transformed into Col-0 plants to develop *AtWRKY75* overexpression lines following floral dip transformation method (Clough and Bent, 1998).*pPHT1;5*::*GUS* recombinant construct was similarly transformed into *wrky75* mutant line. The vector control lines harboring the *CaMV35S::GUS* construct was generated in the background of Col-0 as well as *wrky75* mutant. The putative transformants were selected by antibiotic screening (kanamycin for *pPHT1;5*::*GUS*, and *pPHT1;5*::*PHT1;5* whereas hygromycin for*CaMV35S::WRKY75-HA*and *CaMV35S::GUS*) and positive plants were selected by selectable marker specific PCR amplification. The selected plants were grown up to T_2 generation in a growth chamber as described above.

Histochemical GUS assay

The 7 d old seedlings from transgenic lines (T_2 generation) harboring the *pPHT1;5*::*GUS*, and *CaMV35S::GUS* constructs (in the background of Col-0 and *wrky75* mutant) were maintained under +P or -P conditions or treated with exogenous GSH as described above. The samples were then infiltrated with GUS staining solution (0.5 mg mL^{-1} 5-bromo-4-chloro-3-indolylβ-D-glucuronic acid, 0.5 mM potassium ferrocyanide, 0.5 mM potassium ferricyanide, 0.1% [v/v] Triton X-100, 100 mM phosphate buffer, pH 7.0, and 10 mM EDTA) and histochemical GUS assay was performed following Jefferson et al.(1987). Samples were washed with 70% alcohol and photographed.

Y1H analysis

The PCR amplified promoter sequence of *AtPHT1;5* gene was cloned into *pAbAi* vector (Takara) between the *SacI* and *KpnI* RE sites following manufacturer's protocol. The cds of *AtWRKY6*, *AtWRKY42*, *AtWRKY45*, *AtWRKY75*, *AtMYB2*, and *AtMYB62* genes were amplified by PCR using gene specific primers and cloned into *pGADT7-Rec* vector (Takara). The recombinant constructs were transformed into Y1H gold strain (Takara). The transformed yeast strains were grown on SD/-Leu and SD/-Leu/AureobasidinA media (Takara) and Y1H analysis was performed using Matchmaker® Gold Yeast One-hybrid screening system (Takara) according to the manufacturer's protocol. The interaction between p53-pAbAi was used as positive control and pAbAi alone was considered as negative control.

Dual luciferase transactivation assay

The promoter region of *AtPHT1;5* was cloned into *pGreen-LUC008* vector between *SpeI* and *KpnI* RE sites to drive the expression of firefly luciferase gene expression. The construct constitutively expressing Renilla luciferase (*REN*) gene and harbouring *pPHT1;5::LUC* cassette was used as reporter. The *CaMV35S::WRKY75-HA* construct was considered as effector. *Agrobacterium* strains harboring the recombinant constructs (effecter and reporter) were mixed in 1:1 ratio (v/v) and used for *Agrobacterium*-mediated infiltration of *Nicotiana tabaccum* leaves (Sahid et al., 2020). For negative control, *Agrobacterium* strain harboring the effector construct and empty *pGreen-LUC008* vector were mixed into 1:1 ratio (v/v) and used for infiltration (Zhang et al., 2015). After incubation for 48h at dark, infiltrated leaves were harvested and total protein was isolated. 1 µg protein was used for dual luciferase transactivation assay using Dual-Luciferase® Reporter Assay System (Promega) following manufacturer's protocol. The luminescence was measured using the Varioskan LUX luminometer (Thermo scientific) and relative luciferase activity was calculated using the relative LUC/REN ratio.

CHIP-qPCR analysis

The *CaMV35S::WRKY75-HA* harboring transgenic line was used for ChIP assay following Cheng et al. (2020) with slight modifications. Briefly, 7 d old seedlings were maintained under +P or -P conditions or treated with exogenous GSH as described above. 800 mg tissue from each sample was harvested, washed with milliQ water, cross-linked with 1% (v/v) formaldehyde solution under vacuum for 10 min, and homogenized in liquid nitrogen. The

chromatin complex was isolated, and sheared by sonication (Hielscher Ultrasonic processor, UP200S). The complex was then incubated with 2 µg of anti-HA antibody (Sigma). The precipitated DNA was recovered and ChIP qPCR was performed using EpiQuik™ Chromatin Immunoprecipitation (ChIP) Kit (Epigentek). For the negative control, non-immune IgG antibody was used. The real time PCR was performed in triplicate using CFX96 Touch™ Real-Time PCR Detection System (Bio-rad) using iTaq™ Universal SYBR® Green Supermix (Bio-rad) and two sets of w-box specific primers of *AtPHT1;5* promoter. The chromatin without any antibody treatment was used as input DNA. The %input was calculated from Ct values.

In silico promoter analysis

The presence of w-box motif was identified in the promoter region of *AtPHT1;5* using PlantPan 3.0 (plantpan.itps.ncku.edu.tw/promoter.php) and MEME suite 5.3.3 (https://memesuite.org/).

Statistical analysis

The data was statistically analyzed using GraphPad Prism version 8.3.0 software (GraphPad Software, San Diego, California USA). The variation of morphological and biochemical parameters, as well as relative transcript abundance, were evaluated using one-way ANOVA (Fig. 3A-B,E-L, 5)or two-way ANOVA (Fig. 1, 2, 3C-D, 4, 6B-C, E, G) followed by Dunnett's multiple comparison tests. To determine the difference between two sets of data, statistical significance at $P \leq 0.05$ was used. Details of statistical tests, replicates, sample size, and the significance levels of P-values were indicated in respective figure legends. The data was provided as mean ± standard error of mean (SEM).

Conflict of interest

Authors declare no conflict of interest.

Author Contributions

RD and SP conceived and designed the research plan; RS performed most of the experiments; DS performed *in silico* analysis and Y1H analysis, SS generated the constructs, RD and SP analyzed the data and prepared the manuscript.

Acknowledgement

We thank the central instrumentation facilities of the Department of Botany, and Department of Biochemistry, University of Calcutta and Department of Botany, Dr A. P. J. Abdul Kalam Government College. RS acknowledges the University Research Fellowship, University of Calcutta for her fellowship.

Supplemental information

FIGURE S1 Response of *pad2-1* mutant in response to exogenous GSH feeding.

FIGURE S2 Position of the w-box motifs on the *AtPHT1;5* promoter.

TABLE S1 List of primers used.

References

Anderson ME (1985) Determination of glutathione and glutathione disulfide in biological samples. Methods in Enzymology **113**: 548–555

Ayadi A, David P, Arrighi AF, Chiarenza S, Thibaud MC, Nussaume L, Marin E (2015) Reducing the genetic redundancy of Arabidopsis PHOSPHATE TRANSPORTER1 transporters to study phosphate uptake and signaling. Plant Physiology **167 (4)**: 1511-1526

Baek D, Park HC, Kim MC, Yun DJ (2013) The role of Arabidopsis MYB2 in miR399f-mediated phosphate-starvation response. Plant Signaling& Behavior**8**: e23488

Bieleski RL (1973) Phosphate pools, phosphate transport, and phosphate availability. Annual review of plant physiology**241(1)**: 225–252

Bucher M, Rausch C, DaramP(2001) Molecular and biochemical mechanisms of phosphorus uptake into plants. Journal of Plant Nutrition and Soil Science **164**: 209– 217

Chen YF, Li LQ, Xu Q, Kong YH, Wang H, Wu WH (2009) The WRKY6 transcription factor modulates PHOSPHATE1 expression in response to low Pi stress in *Arabidopsis*. Plant Cell **21**: 3554–3566

Chen PS, Toribara TY, Warner H (1956) Microdetermination of Phosphorus. Analytical Chemistry**28 (11)**: 1756–1758

Cheng M-C, Enderle B, Kathare PK, Islam R, Hiltbrunner A, Huq E (2020) PCH1 and PCHL directly interact with PIF1, promote its degradation, and inhibit its transcriptional function during photomorphogenesis. Molecular Plant **13(3)**: 499-514

Clough SJ, Bent AF (1998) Floral dip: a simplified method for Agrobacterium□mediated transformation of Arabidopsis thaliana. The Plant Journal **16**: 735–743.

Datta R, Kumar D, Sultana A, Hazra S, Bhattacharyya D, Chattopadhyay S(2015) Glutathione regulates 1□aminocyclopropane□1□carboxylate synthase transcription via WRKY33 and 1□aminocyclopropane□1□carboxylate oxidase by modulating messenger RNA stability to induce ethylene synthesis during stress. Plant Physiology **169**: 2963–2981

Devaiah BN, Madhuvanthi R, Karthikeyan AS, Raghothama KG (2009) Phosphate starvation responses and gibberellic acid biosynthesis are regulated by the MYB62 transcription factor in Arabidopsis. Molecular Plant: 43-58

Devaiah BN, Karthikeyan AS, Raghothama KG (2007) WRKY75 transcription factor is a modulator of phosphate acquisition and root development in Arabidopsis. Plant Physiology **143**:1789-1801

Foyer CH, Noctor G (2011) Ascorbate and Glutathione: The Heart of the Redox Hub. Plant Physiology **155**: 2-18

Glazebrook J, Ausubel FM (1994) Isolation of phytoalexin□deficient mutants of Arabidopsis thaliana and characterization of their interactions with bacterial pathogens. Proceedings of the National Academy of Sciences of the United States of America **91**: 8955–8959

Gu M, Chen A, Sun S, Xu G (2016) Complex regulation of plant phosphate transporters and the gap between molecular mechanisms and practical application: What is missing? Molecular Plant **9**: 396–416

Hernández I, Munné-Bosch S (2015) Linking phosphorus availability with photo-oxidative stress in plants Journal of Experimental Botany**66 (10)**: 2889–2900

Howden R, Goldsbrough PB, Anderson CR, Cobbett CS (1995) Cadmium-sensitive, cad1 mutants of Arabidopsis thaliana are phytochelatin deficient. Plant Physiology**107**:1059–1066

Jefferson RA, Kavangh TA, Bevan MW (1987) Gus fusions: β glucuronidase as a sensitive and versatile gene fusion marker in higher plants. The EMBO Journal **6**: 3901–3907

Jozefczak M, Keunen E, Schat H, Bliek M, Hernandez EL, Carleer R, RemansT, Bohler S, Vangronsveld J, Cuypers A (2014) Differential response of Arabidopsis leaves and roots to cadmium: Glutathione-related chelating capacity vs antioxidant capacity. Plant Physiology and Biochemistry **83**, 1-9

Lapis-Gaza HR, Jost R, Finnegan PM (2014) Arabidopsis PHOSPHATE TRANSPORTER1 genes PHT1;8 and PHT1;9 are involved in root-to-shoot translocation of orthophosphate BMC Plant Biology **14**: 334

Lichtenthaler HK (1987) Chlorophylls and carotenoids: pigments of photosynthetic biomembranes. Methods in Enzymology**148**: 350–382.

Liu B, Zhao S, Wu X, Wang X, Nan Y, Wang DD, Chen Q (2017) Characterization of phosphate transporter genes in potato.Journal of Biotechnology**264**: 17-28

Liu F, Xu Y, Jiang H, Jiang C, Du Y, Gong C, Wang W, Zhu S, Han G, Cheng B (2016) Systematic identification, evolution and expression analysis of the Zea mays PHT1 gene family reveals several new members involved in root colonization by arbuscularmycorrhizal fungi. International Journal of Molecular Science **17**: 930

Marschner H (2012) Mineral Nutrition of Higher Plants Academic Press London.

Marschner H, Marschner P (2012) Marschner's Mineral Nutrition of Higher Plants (3rd edn.). Elsevier Academic Press San Diego USA: 1–651

Matsui K, Tanaka H, Ohme-Takagi M (2004) Suppression ofthe biosynthesis of proanthocyanidin in Arabidopsis by a chimericPAP1 repressor. Plant Biotechnololy Journal**2**: 487–493.

Mudge SR, Rae AL, Diatloff E, Smith FW (2002) Expression analysis suggests novel roles for members of the Pht1 family of phosphate transporters in Arabidopsis. The Plant Journal **31**: 341-353

Murashige T, Skoog F (1962) A revised medium for rapid growth and bioassays with tobacco tissue cultures. PhysiologiaPlantarum**15**: 473–497

Nagarajan VK, Jain A, Poling MD, Lewis AJ, Raghothama KG, Smith AP (2011) Arabidopsis Pht1;5 mobilizes phosphate betweensource and sink organs and influences the interaction between phosphate homeostasis and ethylene signaling. Plant Physiology**156**: 1149–1163

Noctor G, Mhamdi A, Chaouch S, Han Y, Neukermans J, Marquez-Garcia B, Queval G, Foyer CH (2012) Glutathione in plants: an integrated overview. Plant Cell & Environment 35 (2): 454-84

Parisy V, Poinssot B, Owsianowski L, Buchala A, Glazebrook J, Mauch F (2007) Identification of PAD2 as a gamma□glutamyl cysteine synthetase highlights the importance of glutathione in disease resistance of Arabidopsis. The Plant Journal **49**: 159–172

Péret B, Desnos T, Jost R, Kanno S, Berkowitz O, Nussaume L (2014) Root Architecture Responses: In Search of Phosphate. Plant Physiology **166**: 1713–1723

Poirier Y, Bucher M (2002) Phosphate Transport and Homeostasis in Arabidopsis. The Arabidopsis Book **1**: e0024

Raghothama KG (1999) Phosphate acquisition. Annual Review of Plant Physiology Plant Molecular Biology **50**: 665–693

Rubio V, Linhares F, Solano R, Martín AC, Iglesias J, Leyva A, Paz-Ares A (2001) A conserved MYB transcription factor involved in phosphate starvation signaling both in vascular plants and in unicellular algae. Genes & Development **15 (16)**: 2122-2133

Sahid S, Roy C, Paul S, Datta R (2020) Rice lectin protein r40c1 imparts drought tolerance by modulating S-adenosylmethionine synthase 2, stress associated protein 8 and chromatin associated proteins. Journal of Experimental Botany **71 (22)** 7331–7346

Seth CS, Remans T, Keunen E, Jozefczak M, Gielen H, Opdenakker K, Weyens N, Vangronsveld J, Cuypers A (2012) Phytoextraction of toxic metals: a central role for glutathione. Plant Cell & Environment **35**: 334-346

Shanmugam V, Tsednee M, Yeh KC (2012) Zinc tolerance induced by iron 1 reveals the importance of glutathione in the cross□homeostasis between zinc and iron in Arabidopsis thaliana. The Plant Journal **69**:1006–1017

Shanmugam V, Wang YW, Tsednee M, Karunakaran K, Yeh KC (2015) Glutathione plays an essential role in nitric oxide mediated iron deficiency signaling and iron deficiency tolerance in Arabidopsis. The Plant Journal **84**: 464–477

Shee R, Ghosh S, Khan P, Sahid S, Roy C, Shee D, Paul S, Datta R (2022) Glutathione regulates transcriptional activation of iron transporters via S-nitrosylation of bHLH factors to modulate subcellular iron homoeostasis. Plant Cell & Environment **45**: 2176-2190

Shin H, Shin HS, Dewbre GR, Harrison MJ (2004) Phosphate transport in Arabidopsis: Pht1;1 and Pht1;4 play a major role in phosphate acquisition from both low- and high-phosphate environments. The Plant Journal **39**: 629–642

Sinha R, Kumar D, Datta R, Hazra S, Bhattacharyya D, Mazumdar AB, Mukhopadhyay R, Sultana A, Chattopadhyay S (2014) Integrated transcriptomic and proteomic analysis of *Arabidopsis thaliana* exposed to glutathione unravels its role in plant defense. Plant Cell Tissue and Organ Culture **120**: 975–988

Trujillo-Hernandez JA, Bariat L, Enders TA, Strader LC, Reichheld JP, Belin C (2020) A glutathione-dependent control of the indole butyric acid pathway supports Arabidopsis root system adaptation to phosphate deprivation. Journal of Experimental Botany **71(16)**: 4843–4857

van der Graaff E, Schwacke R, Schneider A,Desimone M, Flugge UI, Kunze R(2006) Transcription analysis of Arabidopsis membrane transporters and hormone pathways during developmental and induced leaf senescence. Plant Physiology **141**: 776–792

Vance CP, Uhde-Stone C, Allan DL (2003) Phosphorus Acquisition and Use: Critical Adaptations by Plants for Securing a NonrenewableResource.New Phytologist**157**: 423-447

Wang L, Li Z, Qian W, Guo W, Gao X, Huang L, Wang H, Zhu H, Wu JW, Wang D, Liu D (2011) The Arabidopsis purple acid phosphatase AtPAP10 is predominantly associated with the root surface and plays an important role in plant tolerance to phosphate limitation. Plant Physiology **157**: 1283-1299

Wang H, **Xu Q**, **Kong YH**, **Chen Y**, **Duan JY**, **Wu WH**, **Chen YF** (2014) Arabidopsis WRKY45 transcription factor activates PHOSPHATE TRANSPORTER1;1 expression in response to phosphate starvation. Plant Physiology **164**: 2020– 2029

Williamson LC, Ribrioux SP, Fitter AH, Leyser HM (2001) Phosphate availability regulates root system architecture in Arabidopsis. Plant Physiology **126**: 875–882

Zhang F, Fu X, Lv Z, Lu X, Shen Q, Zhang L, Zhu M, Wang G, Sun X, Liao Z, Tang K (2015) A basic leucine zipper transcription factor, AabZIP1, connects abscisic acid signaling with artemisinin biosynthesis in *Artemisia annua*. Molecular Plant **8**: 163–175

Zhang F, Wu XN, Zhou HM, Wang DF, Jiang TT, Sun YF, Cao Y, Pei WX, Sun SB, Xu GH (2014) Overexpression of rice phosphate transporter gene OsPT6 enhances phosphate uptake and accumulation in transgenic rice plants. Plant and Soil **384**: 259–270

Figure Legends

FIGURE 1 Response of GSH-deficient mutants to Pi starvation. 7 d old MS grown seedlings of Col-0, *cad2-1* and *pad2-1*were exposed to +P and -P conditions for 7 d and analyzed. (A) Representative images of plants grown under +P and –P conditions, (B) rosette diameter, (C) primary root length, (D) lateral root number, (E) lateral root density, (F) chlorophyll content, and (G) anthocyanin content. The experiment was independently repeated thrice and results were represented as mean±SEM (n=15). Statistical differences between the genotypes were analyzed by two-way ANOVA followed by Dunnett's multiple comparison test and statistical significances were denoted by asterisks in the respective panels.

FIGURE 2 Estimation of Pi and total P contents, total GSH and GSH:GSSG ratio under +P and -P conditions. 7 d old MS grown Col-0, *cad2-1* and *pad2-1*seedlings were exposed to -P condition for 7 d and analyzed. Control plants were maintained in the MS medium for the entire period. (A) Root Pi content, (B) total root P content (C) total root GSH content, (D) root GSH:GSSG ratio, (E) shoot Pi content, (F) total shoot P content, (G) total shoot GSH content, and (H) shoot GSH:GSSG ratio. The experiment was independently repeated thrice and results were represented as mean±SEM (n=9). Statistical differences between the genotypes were analyzed by two-way ANOVA followed by Dunnett's multiple comparison test and statistical significances were denoted by asterisks in the respective panels.

FIGURE 3 Expression analyses of different P transporters under altered GSH conditions. 14 d old MS grown Col-0, *cad2-1*, and *pad2-1* plants were analyzed for the expression pattern of various P transporter genes. Expression of different P transporters from root (A) and shoot (B) tissues was depicted as heat map. Relative transcript abundance of *AtPHT1;5* gene was analyzed from root (C) and shoot (D) of 7 d old Col-0, *cad2-1*, and *pad2-1*seedlings grown under +P and -P conditions for additional 7 d. 14 d old MS grown Col-0 plants were treated with 100 μM GSH, or 1 mM BSO, or 5 mM DTT solutions and analyzed. Control plants were maintained in half strength MS medium for the entire duration. (E) Total root GSH content, (F)total root P content,(G) root Pi content, (H) relative transcript abundance of *AtPHT1;5*gene in roots, (I) total shoot GSH content, (J) total shoot P content, (K) shoot Pi content and (L) relative transcript abundance of *AtPHT1;5*gene in shoots. The experiment was independently repeated thrice and results were represented as mean±SEM

(n=3). Statistical differences between the genotypes or treatments were analyzed by one-way ANOVA (A,B, E-L) or two-way ANOVA (C-D) followed by Dunnett's multiple comparison test and statistical significances were denoted by asterisks in the respective panels.

FIGURE 4 Response of *pht1;5* mutant and complementation lines to exogenous GSH under Pi-sufficient and Pi-deficient conditions. 7 d old MS grown seedlings of Col-0, *pht1;5* mutant and complementation (*pht1;5/pPHT1;5::PHT1;5*) lines were treated with 100 µM GSH, exposed to +P and -P conditions for 7 d and analyzed. (A) Representative images of plants grown under +P, +P+GSH, -P, and –P+GSH conditions, (B) total root GSH content, (C) root Pi content (D) total root P content, (E) total shoot GSH content, (F) shoot Pi content and (G) total shoot P content. The experiment was independently repeated thrice and results were represented as mean±SEM (n=9). Statistical differences between the genotypes were analyzed by two-way ANOVA followed by Dunnett's multiple comparison test and statistical significances were denoted by asterisks in the respective panels. Scale bar: 10 mm

FIGURE 5 Promoter analysis of the *AtPHT1;5* gene. The seedlings of transgenic lines harboring *pPHT1;5::GUS* construct and the vector control (*35S::GUS*) lines were exposed to +P, –P, and +P+GSH conditions and used for promoter analysis by histochemical GUS assay and qRT-PCR analysis for *GUS (uidA)* gene expression. (A) Representative images of histochemical GUS staining of transgenic line harboring*pPHT1;5::GUS* construct, (B) relative transcript abundance of *GUS* gene of the same, (C) representative images of histochemical GUS staining of vector control line harboring the *35S::GUS* construct(negative control), and(D) relative transcript abundance of *GUS* gene of the same. The experiment was independently repeated thrice. For relative transcript abundance, results were represented as mean±SEM (n=3). Statistical differences between the treatments were analyzed by one-way ANOVA followed by Dunnett's multiple comparison test and statistical significance of relative gene expression was denoted in the respective panels. Scale bar: 5 mm

FIGURE 6 Identification of TFs interacting with *AtPHT1;5* promoter and its regulation by GSH. (A) Y1H analysis for interaction of the P responsive TFs, *At*WRKY6, *At*WRKY42, *AtWRKY45*, *At*WRKY75, *At*MYB2, and *At*MYB62 with the *AtPHT1;5* promoter. (B) Relative transcript abundance of *AtMYB2*, *AtWRKY42* and *AtWRKY75* genes in the Col-0, *cad2-1* and *pad2-1* plants, (C) relative transcript abundance of *AtPHT1;5* gene in theCol-0, *wrky42*, *wrky75*, and *myb2* mutants grown under +P and –P condition. (D) Dual luciferase transctivation assay for *At*WRKY75-*AtPHT1;5* promoter. (E) ChIP-qPCR analysis for

binding of *At*WRKY75 to the *AtPHT1;5* promoter under +P, -P, and +P+GSH conditions. The position of the w-box motifs along with primer positions are marked on the promoter. (F) Promoter analysis of the *AtPHT1;5* gene in the*wrky75* mutant background. Representative images of histochemical GUS staining of the transgenic *wrky75/pPHT1;5::GUS* and *wrky75/35S::GUS* (vector control) lines grown under +P, -P and +P+GSH conditions. (G) Relative transcript abundance of *GUS* (*uidA*) gene of the same. The experiment was independently repeated thrice and results were represented as mean±SEM (n=3). Statistical differences between the treatments (B-C, E, G) were analyzed by one-way ANOVA followed by Dunnett's multiple comparison test or student t test (D) and statistical significance was denoted in the respective panels.

FIGURE 7 Proposed model for GSH mediated regulation of P translocation under Pi-limited condition. Pi deficiency leads to the accumulation of GSH in cells which then activates the P transporter, *AtPHT1;5* and increase source to sink P distribution. This GSH mediated regulation involves transcriptional induction of the *AtPHT1;5* gene via the P-responsive *At*WRKY75 TF.

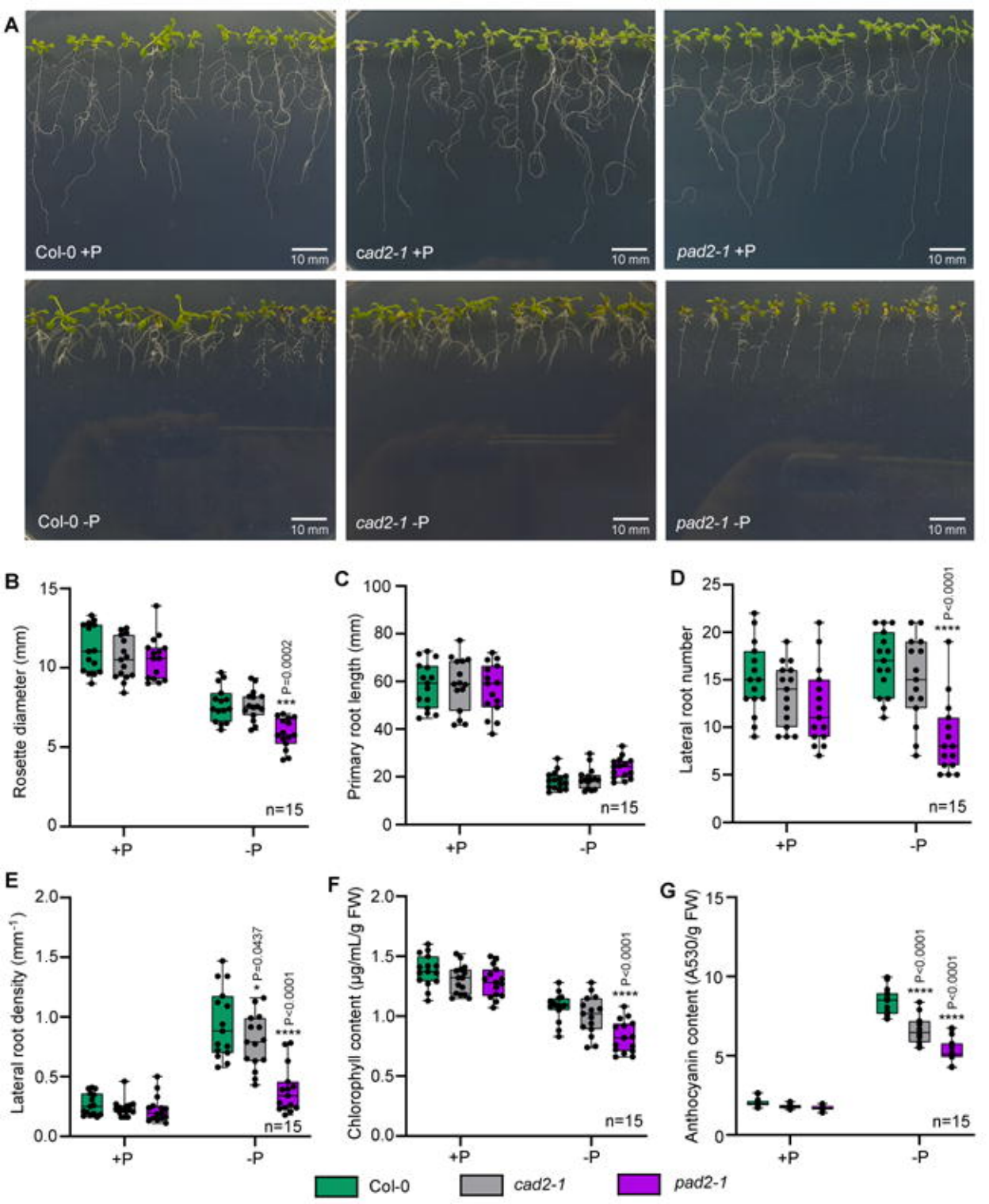
A
Col-0 +P
cad2-1 +P
pad2-1 +P
Col-0 -P
cad2-1 -P
pad2-1 -P
10 mm
B
Rosette diameter (mm)
** P=0.0002
n=15
C
Primary root length (mm)
n=15
D
Lateral root number
**** P<0.0001
n=15
E
Lateral root density (mm⁻¹)
* P=0.0437
**** P<0.0001
n=15
F
Chlorophyll content (µg/mL/g FW)
**** P<0.0001
n=15
G
Anthocyanin content (A530/g FW)
**** P<0.0001
**** P<0.0001
n=15
+P
-P
Col-0
cad2-1
pad2-1

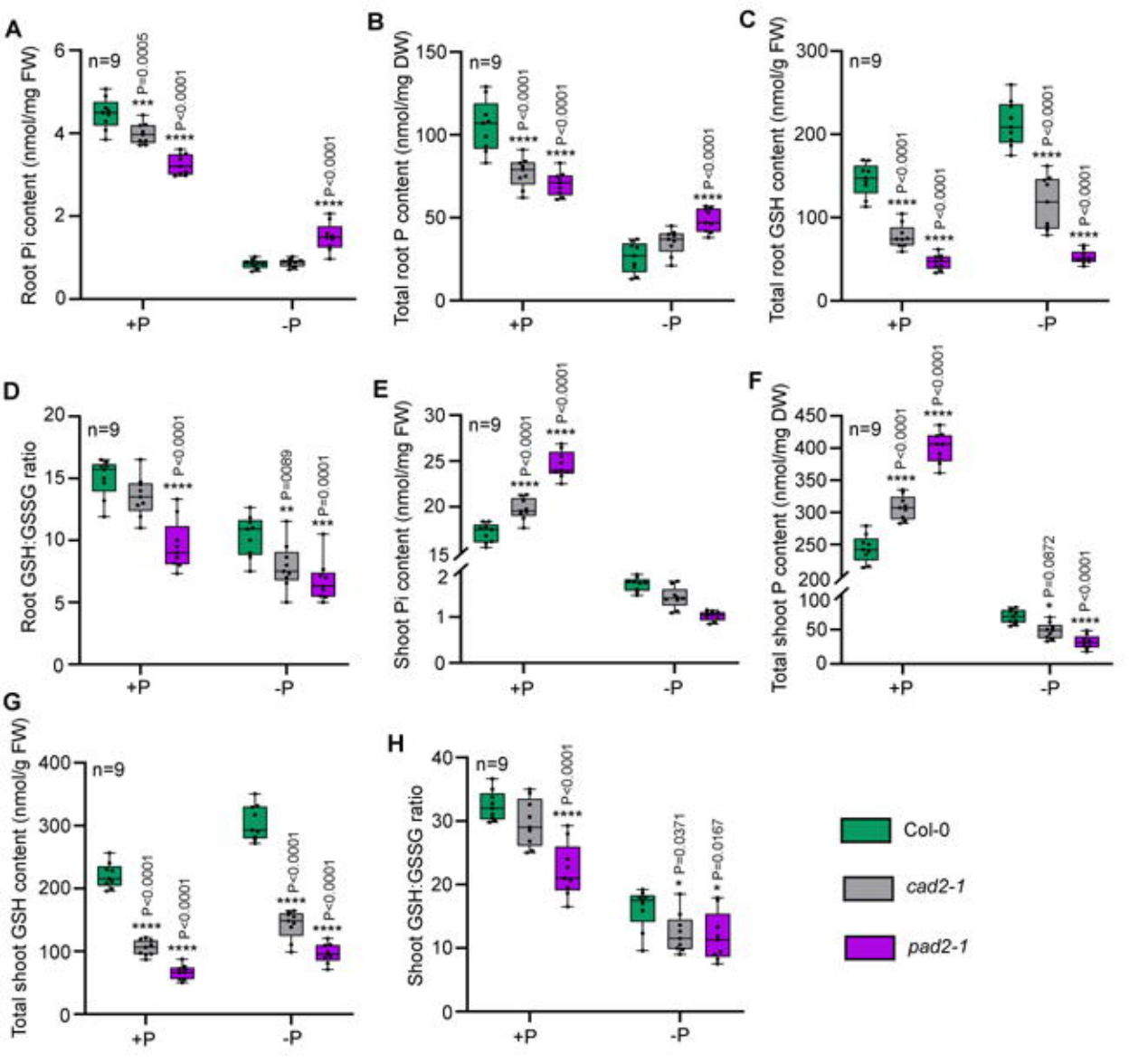
A
Root Pi content (nmol/mg FW)
n=9
P=0.0005
P<0.0001
P<0.0001
+P
-P
B
Total root P content (nmol/mg DW)
n=9
P<0.0001
P<0.0001
P<0.0001
+P
-P
C
Total root GSH content (nmol/g FW)
n=9
P<0.0001
P<0.0001
P<0.0001
P<0.0001
+P
-P
D
Root GSH:GSSG ratio
n=9
P<0.0001
P=0.0089
P=0.0001
+P
-P
E
Shoot Pi content (nmol/mg FW)
n=9
P<0.0001
P<0.0001
+P
-P
F
Total shoot P content (nmol/mg DW)
n=9
P<0.0001
P<0.0001
P=0.0872
P<0.0001
+P
-P
G
Total shoot GSH content (nmol/g FW)
n=9
P<0.0001
P<0.0001
P<0.0001
P<0.0001
+P
-P
H
Shoot GSH:GSSG ratio
n=9
P<0.0001
P=0.0371
P=0.0167
+P
-P
Col-0
cad2-1
pad2-1

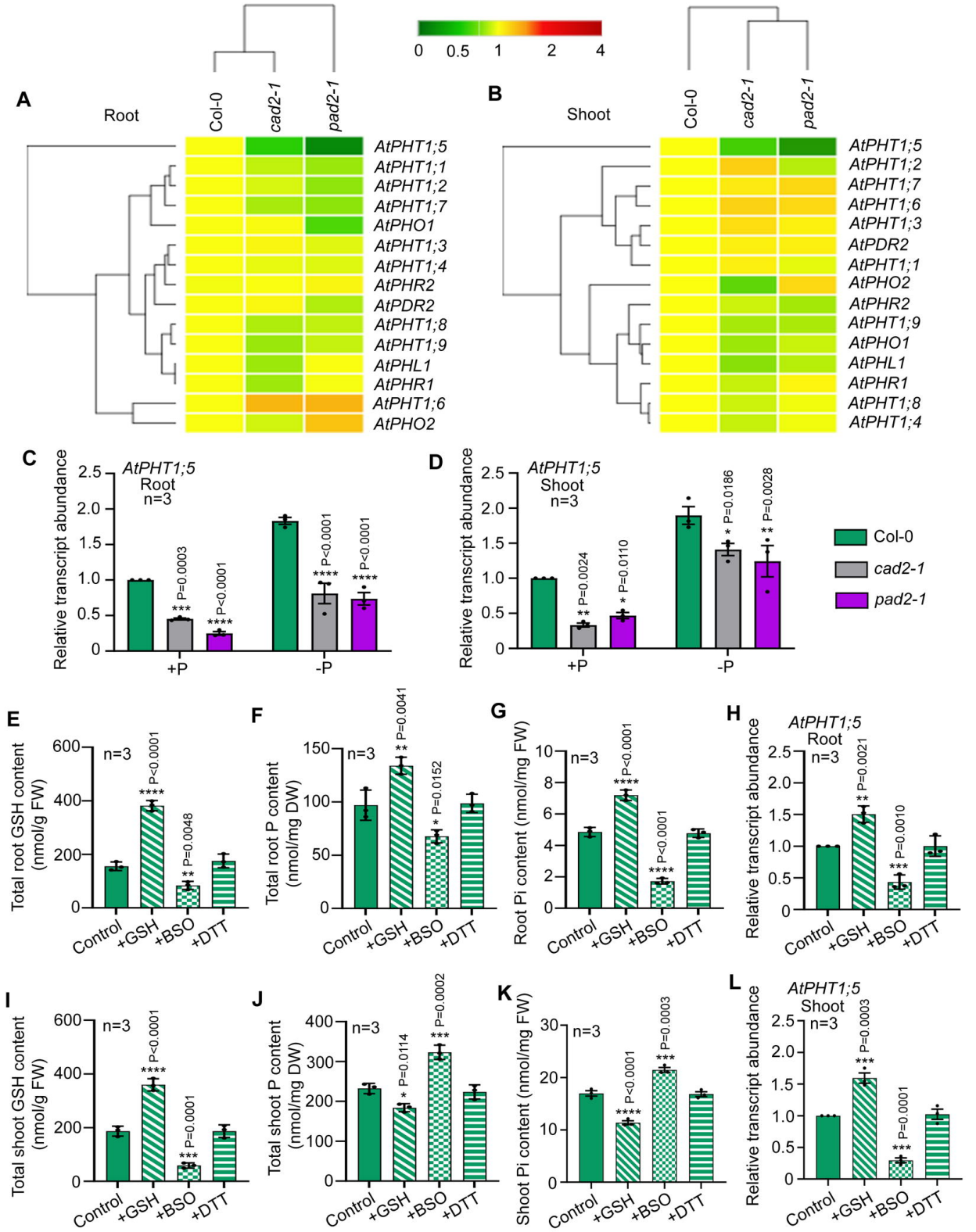
0 0.5 1 2 4
A
Root
Col-0
cad2-1
pad2-1
AtPHT1;5
AtPHT1;1
AtPHT1;2
AtPHT1;7
AtPHO1
AtPHT1;3
AtPHT1;4
AtPHR2
AtPDR2
AtPHT1;8
AtPHT1;9
AtPHL1
AtPHR1
AtPHT1;6
AtPHO2
B
Shoot
Col-0
cad2-1
pad2-1
AtPHT1;5
AtPHT1;2
AtPHT1;7
AtPHT1;6
AtPHT1;3
AtPDR2
AtPHT1;1
AtPHO2
AtPHR2
AtPHT1;9
AtPHO1
AtPHL1
AtPHR1
AtPHT1;8
AtPHT1;4
C
AtPHT1;5
Root
n=3
Relative transcript abundance
P=0.0003
P<0.0001
P<0.0001
P<0.0001
+P
-P
D
AtPHT1;5
Shoot
n=3
Relative transcript abundance
P=0.0024
P=0.0110
P=0.0186
P=0.0028
+P
-P
Col-0
cad2-1
pad2-1
E
Total root GSH content (nmol/g FW)
n=3
P<0.0001
P=0.0048
Control
+GSH
+BSO
+DTT
F
Total root P content (nmol/mg DW)
n=3
P=0.0041
P=0.0152
Control
+GSH
+BSO
+DTT
G
Root Pi content (nmol/mg FW)
n=3
P<0.0001
P<0.0001
Control
+GSH
+BSO
+DTT
H
AtPHT1;5
Root
n=3
Relative transcript abundance
P=0.0021
P=0.0010
Control
+GSH
+BSO
+DTT
I
Total shoot GSH content (nmol/g FW)
n=3
P<0.0001
P=0.0001
Control
+GSH
+BSO
+DTT
J
Total shoot P content (nmol/mg DW)
n=3
P=0.0114
P=0.0002
Control
+GSH
+BSO
+DTT
K
Shoot Pi content (nmol/mg FW)
n=3
P<0.0001
P=0.0003
Control
+GSH
+BSO
+DTT
L
AtPHT1;5
Shoot
n=3
Relative transcript abundance
P=0.0003
P=0.0001
Control
+GSH
+BSO
+DTT

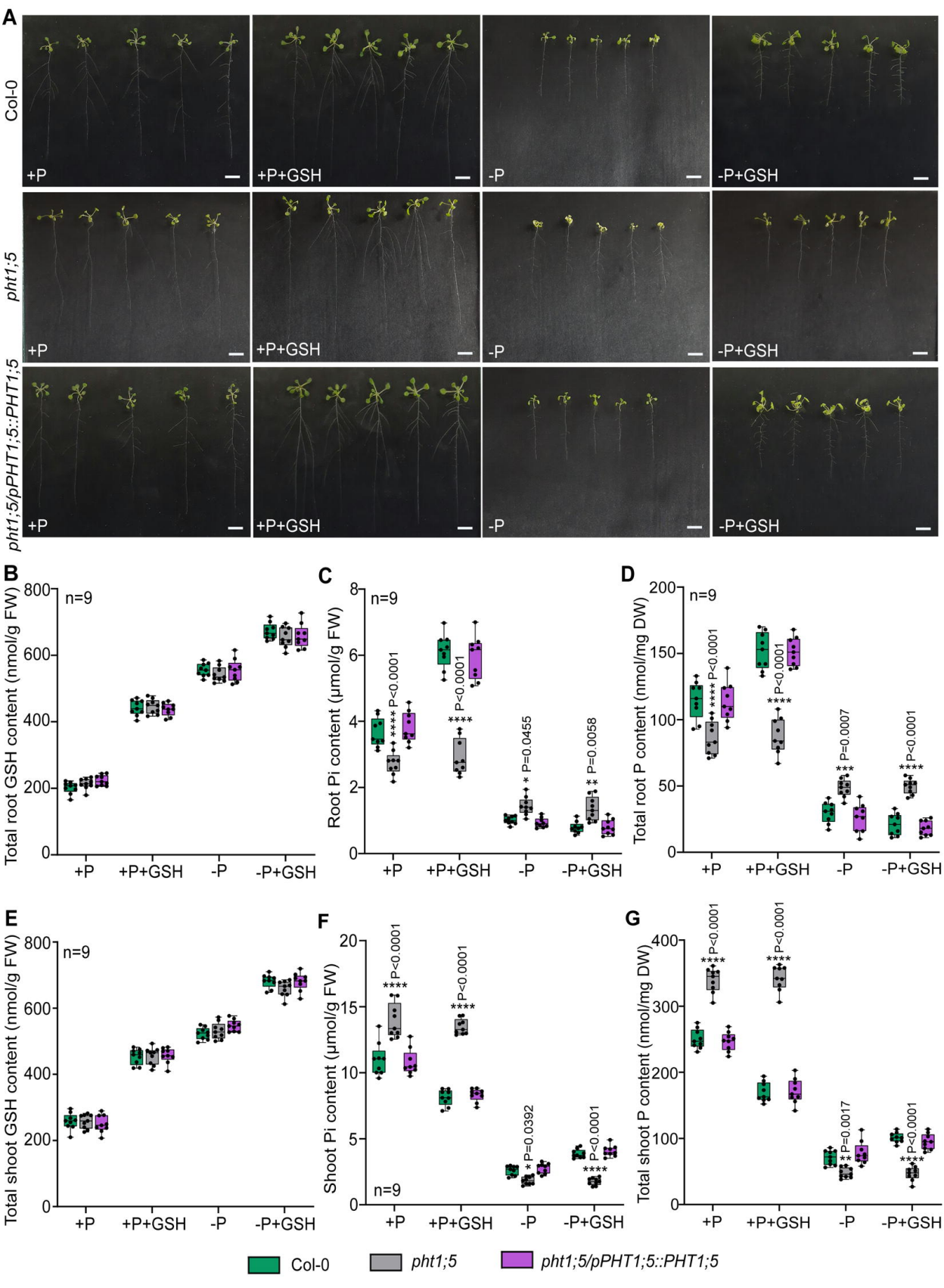
A
Col-0
pht1;5
pht1;5/pPHT1;5::PHT1;5
+P
+P+GSH
-P
-P+GSH
B
Total root GSH content (nmol/g FW)
n=9
C
Root Pi content (µmol/g FW)
n=9
D
Total root P content (nmol/mg DW)
n=9
E
Total shoot GSH content (nmol/g FW)
n=9
F
Shoot Pi content (µmol/g FW)
n=9
G
Total shoot P content (nmol/mg DW)
P<0.0001
P=0.0455
P=0.0058
P=0.0007
P=0.0392
P=0.0017
Col-0
pht1;5
pht1;5/pPHT1;5::PHT1;5

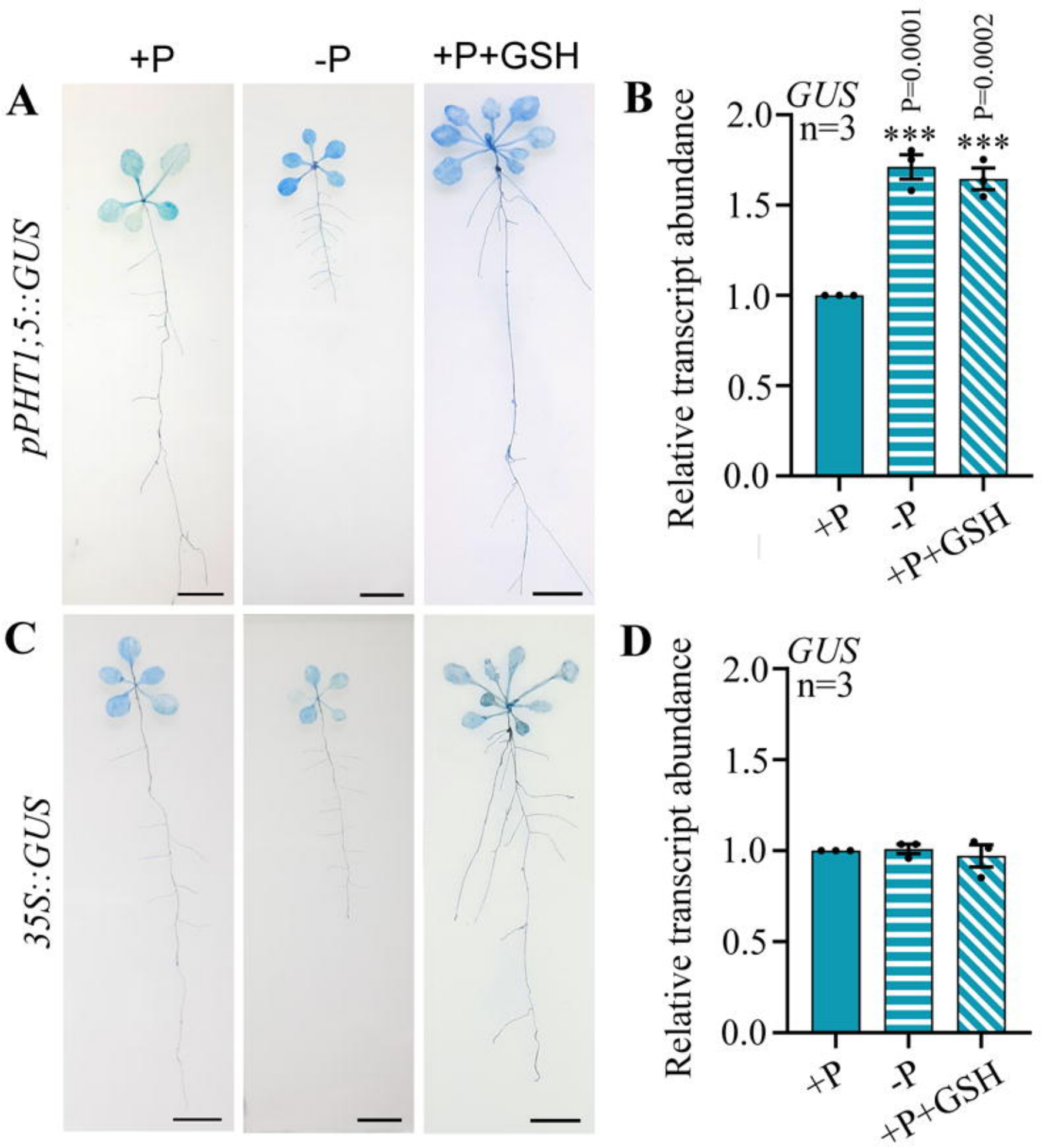
+P
-P
+P+GSH
A
pPHT1;5::GUS
B
GUS
n=3
P=0.0001
P=0.0002
***
***
Relative transcript abundance
2.0
1.5
1.0
0.5
0.0
+P
-P
+P+GSH
C
35S::GUS
D
GUS
n=3
Relative transcript abundance
2.0
1.5
1.0
0.5
0.0
+P
-P
+P+GSH

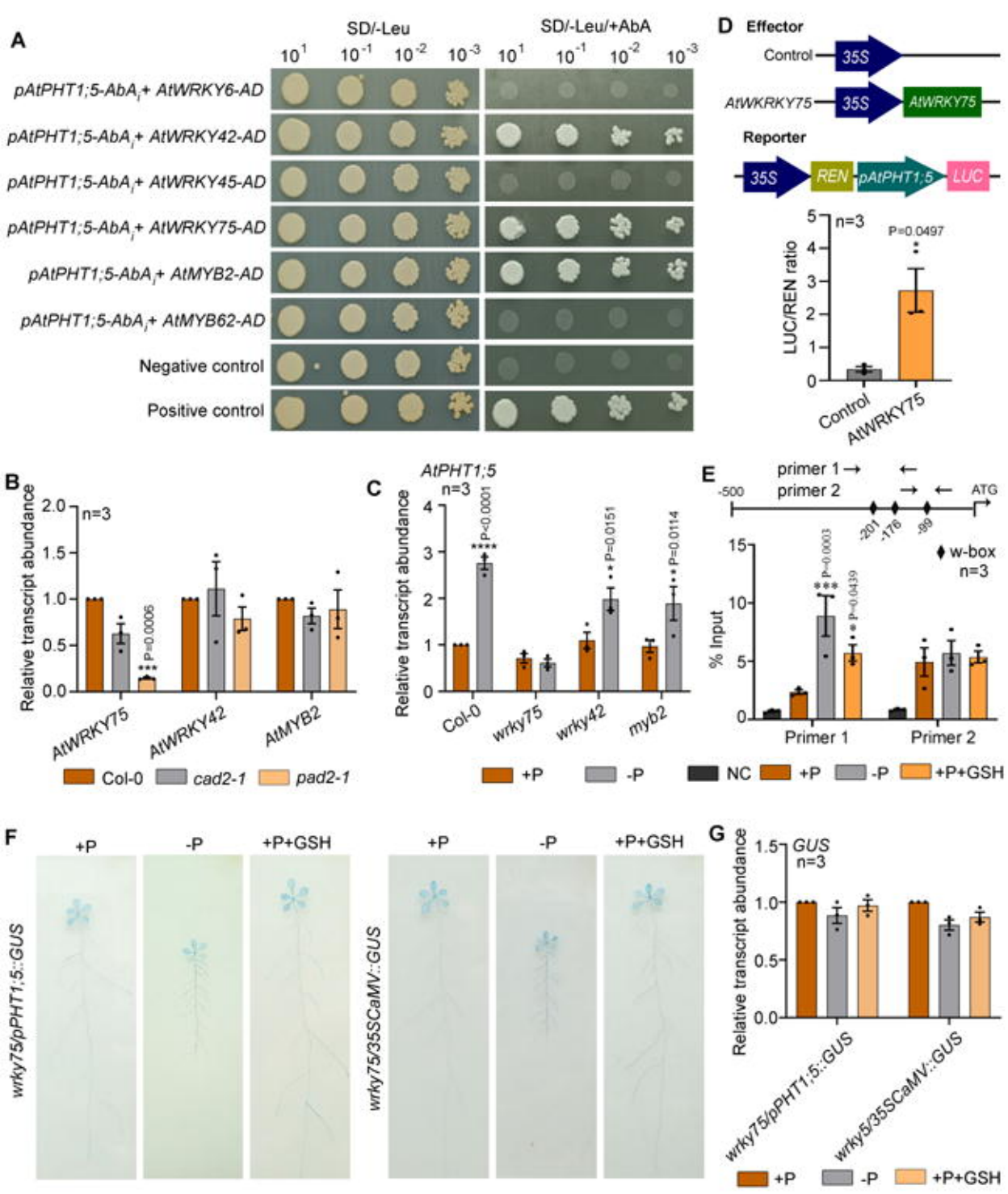
A
SD/-Leu
SD/-Leu/+AbA
10^1 10^-1 10^-2 10^-3
pAtPHT1;5-AbAi+ AtWRKY6-AD
pAtPHT1;5-AbAi+ AtWRKY42-AD
pAtPHT1;5-AbAi+ AtWRKY45-AD
pAtPHT1;5-AbAi+ AtWRKY75-AD
pAtPHT1;5-AbAi+ AtMYB2-AD
pAtPHT1;5-AbAi+ AtMYB62-AD
Negative control
Positive control
D
Effector
Control
35S
AtWKRKY75
AtWRKY75
Reporter
35S
REN
pAtPHT1;5
LUC
n=3
P=0.0497
LUC/REN ratio
Control
AtWRKY75
B
n=3
Relative transcript abundance
P=0.0006
AtWRKY75
AtWRKY42
AtMYB2
Col-0
cad2-1
pad2-1
C
AtPHT1;5
n=3
Relative transcript abundance
P<0.0001
P=0.0151
P=0.0114
Col-0
wrky75
wrky42
myb2
+P
-P
E
primer 1
primer 2
-500
ATG
-201
-176
-99
w-box
n=3
% Input
P=0.0003
P=0.0439
Primer 1
Primer 2
NC
+P
-P
+P+GSH
F
+P
-P
+P+GSH
wrky75/pPHT1;5::GUS
wrky75/35SCaMV::GUS
G
GUS
n=3
Relative transcript abundance
wrky75/pPHT1;5::GUS
wrky5/35SCaMV::GUS
+P
-P
+P+GSH

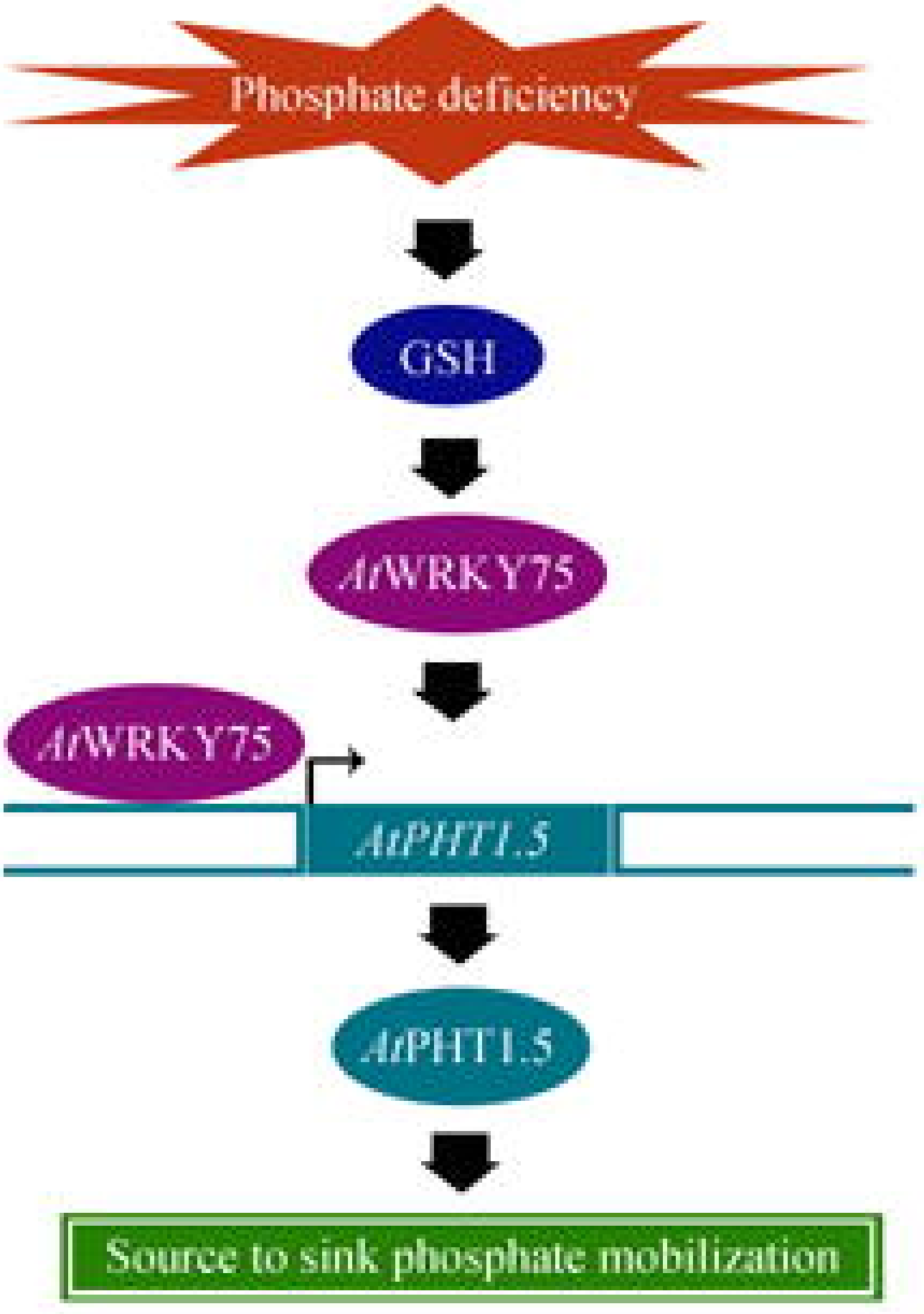
Phosphate deficiency
GSH
AtWRKY75
AtWRKY75
AtPHT1.5
AtPHT1.5
Source to sink phosphate mobilization